

# Influence of Extrusion, Stretching and Poling on the Structural and Piezoelectric Properties of Poly (vinylidene fluoride-hexafluoropropylene) Copolymer Films

Yan Huan,<sup>1,2</sup> Yayan Liu,<sup>1</sup> Yifei Yang,<sup>1,2</sup> Yanan Wu<sup>1,3</sup>

<sup>1</sup>Green Chemistry and Process Laboratory, Changchun Institute of Applied Chemistry, Chinese Academy of Sciences, Changchun 130022, People's Republic of China

<sup>2</sup>Graduate School, Chinese Academy of Sciences, Beijing 100049, People's Republic of China

<sup>3</sup>Materials Science and Engineering, Jilin University, Changchun 5988, People's Republic of China

Received 30 August 2006; accepted 6 October 2006

DOI 10.1002/app.25603

Published online in Wiley InterScience (www.interscience.wiley.com).

**ABSTRACT:** Three types of poly (vinylidene fluoride-hexafluoropropylene) (PVDF-HFP) copolymer films were prepared by extrusion, stretching as well as simultaneously stretching and static electric field poling (SSSEP), respectively, and measured by the differential scanning calorimetric, wide angle X-ray diffraction, Fourier transformation infrared-attenuated total reflection, and Dynamic mechanical analysis. The experimental results showed that the films prepared by stretching and SSSEP have higher crystallinity and  $\beta$  phase than by extrusion. SSSEP improved the chain orientation enormously both in crystalline and amorphous regions, resulting in the highest storage modulus. Because

of the lower  $\beta$  phase content, the extruded films exhibited the lowest piezoelectric coefficient  $d_{33}$ . For the stretched and SSSEP films, although the  $\beta$  phase content was similar, the  $d_{33}$  was distinct because of the different potential energy for the rotation of the dipoles. In addition, the SSSEP films gave the maximum  $d_{33}$  (24 pC/N), higher than the other PVDF-HFP copolymer films that have been reported. © 2007 Wiley Periodicals, Inc. *J Appl Polym Sci* 104: 858–862, 2007

**Key words:** PVDF-HFP; PVDF poling; extrusion; stretching; piezoelectricity

## INTRODUCTION

Polyvinylidene fluoride (PVDF) and its copolymers have ascendant piezoelectric and ferroelectric properties and were widely studied in the past 40 years.<sup>1–4</sup> At least four crystalline phases,  $\alpha$ ,  $\beta$ ,  $\gamma$ , and  $\delta$ , have been reported in PVDF while the molecular chain conformations of these phases are: *trans-gauche*<sup>+</sup>-*trans-gauche*<sup>-</sup> (TG<sup>+</sup>TG<sup>-</sup>) for  $\alpha$  and  $\delta$  phase, all trans (TTTT) for  $\beta$  phase, and T<sub>3</sub>G<sup>+</sup>T<sub>3</sub>G<sup>-</sup> for  $\gamma$  phase.<sup>2–5</sup> The  $\alpha$  phase is a common phase with a TG<sup>+</sup>TG<sup>-</sup> molecular chain conformation and can be obtained from melt or solvent casting<sup>5–9</sup> and the  $\beta$  phase is the most useful phase, which has aroused more technological interest for providing the piezoelectric and ferroelectric properties. For the excellent piezoelectric and ferroelectric properties,  $\beta$  phase was studied most, the results showed that it can be obtained by transforming from  $\alpha$  phase under special conditions such as, mechanical deformation,<sup>10,11</sup> high electric field,<sup>12,13</sup> quenching,<sup>14</sup> and through the use of nucleating agents.<sup>15</sup> It has been found that  $\beta$  phase of

random copolymers of PVDF with trifluoroethylene (PVDF-TrFE) or tetrafluoroethylene (PVDF-TeFE) can be directly obtained from melt. The Curie transition temperature, which has not been found in the PVDF homopolymer, has also been detected in these copolymers.<sup>2,3</sup> Interestingly, the PVDF-TrFE copolymers exhibited excellent electrostrictive response if irradiated by high energy electron beam.<sup>16,17</sup> Lately, another PVDF copolymers poly (vinylidene fluoride-hexafluoropropylene) (PVDF-HFP) were reported to exhibit giant electrostrictive response when were hot pressed followed by quenched in ice water.<sup>18,19</sup> Piezoelectric coefficient ( $d_{31}$ ) comparable to PVDF and pyroelectric coefficient higher than PVDF were reported on stretched and poled PVDF-HFP films.<sup>20</sup> This indicate that PVDF-HFP copolymers, which are often used in lithium batteries as electrolytes,<sup>21,22</sup> have excellent prospect in piezo- and ferroelectric fields.

The influence of processing conditions on the structural and piezoelectric properties of PVDF-HFP copolymers is not well understand and compared with the comprehensive studies of PVDF homopolymer and PVDF-TrFE copolymers. In this article we investigated the influence of three different processing conditions (extrusion, stretching and SSSEP) on the structural

Correspondence to: Y. Liu (yyliu@ciac.jl.cn).

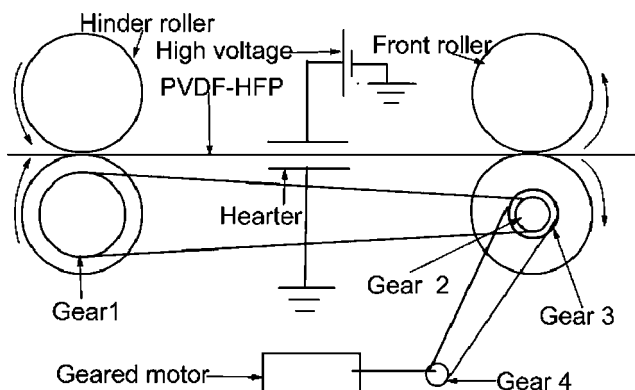


**Figure 1** Apparatus to simultaneously stretch and static electric pole (SSSEP) PVDF-HFP films.

properties and piezoelectricity of PVDF-HFP copolymer with the help of WXAD, FTIR-ATR, DSC, and DMA analytical methods.

## EXPERIMENTAL

### Sample preparation

PVDF-HFP copolymer films of thickness from 30 to 300  $\mu\text{m}$  were prepared by extruding commercial resin (Kynar Flex 2800) with HFP content about 10% by weight. The extruded films were simultaneously stretched and static electric field poled or stretched only, using the apparatus as shown in Figure 1 to make SSSEP films and stretched films, respectively. The similar technique has been used to prepare PVDF piezoelectric films and wonderful results were obtained,<sup>23</sup> here we also gained excellent poled films using the SSSEP technique.

The process of the experiments are depicted as follows: The PVDF-HFP films passed through the hindered rollers, a heated zone, and the front rollers, (the number of gear 1 tooth is 4.5 times of gear 2 tooth, so the speed of the front roller is 4.5 times of the hinder roller's) and were stretched at the heated zone with a fixed stretched ratio 4.5, meanwhile, the high voltage was imposed on the neck-down of the films. The poling of extruded and stretched films are described as: the extruded and stretched films were clamped tightly between two polished sheet coppers, which were placed into a 80°C oven for 20 min with high volts direct current (DC) imposed on the opposite sides.

### Analytical methods

The differential scanning calorimetric (DSC) measurements were carried out in TA2920 equipment, at heating rate of 10°C/min and cooling rate of 20°C/min for all samples. The wide angle X-ray diffractions (WAXD) were performed on Rigaku D/max 2500 diffractometer with Cu K $\alpha$ -Ni radiation. Fourier transformation infrared-attenuated total reflection (FTIR-ATR) spectra were

obtained by a specclamp unit equipped with a 45° ZnSe crystal and recorded with 4  $\text{cm}^{-1}$  resolution using a BRUKER Vertex 70 instrument. Dynamic mechanical analysis (DMA) experiments were taken during a temperature range from -100 to 100°C at a heating rate of 3°C/min and at 20 Hz frequency in a tension-compression mode on the Metravib Mak-04 Viscoanalyser. All films were cut into 5  $\times$  5  $\text{mm}^2$  for stress piezoelectric coefficient  $d_{33}$  measurements, which were carried out in the stress piezoelectric  $d_{33}$  meter (Model ZJ-2, Institute of Acoustics Chinese Academy of Sciences) with frequency of 100 Hz.

## RESULTS AND DISCUSSION

### Structural properties

For DSC measurements, all samples were placed in aluminum pans without constraining and all films shrunk after the measurements. The first run of the heating curves for films prepared under different conditions were shown in Figure 2(a). All films showed similar profiles: a very weak peak at -35°C denoted as glass transition, the main endothermic peak at about 140°C (141°C for extruded films, 143°C for stretched films, and 144°C for SSSEP films) assigned to the melt point. The crystallization enthalpy, which corresponds to the peak area of the exothermic peak, is related to the degree of crystallinity. The SSSEP films exhibited a much larger enthalpy of crystallization (34 J/g) than the stretched (32 J/g) and extruded films (30 J/g). In addition, a small peak appearing at 50°C in the first run but disappearing in the second heating run [Fig. 2(b)] which was immediately followed the first run, has also appeared in DMA results and will be discussed later in this article. In the second run heating diagram [Fig. 2(b)], besides the same  $T_m$  and  $\Delta H$ , all films showed a similar shoulder on the endothermic peak, indicating that the structure of starting films has been entirely altered in to the same structure by first run heating.

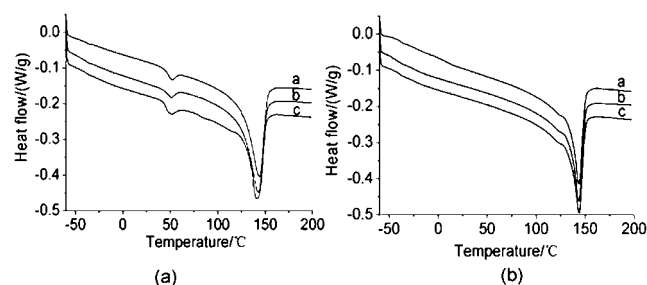


**Figure 2** (a) The first scanning of samples prepared under different conditions. (b) The second scanning of samples prepared under different conditions [(a) SSSEP films, (b) stretched films, (c) extruded films].

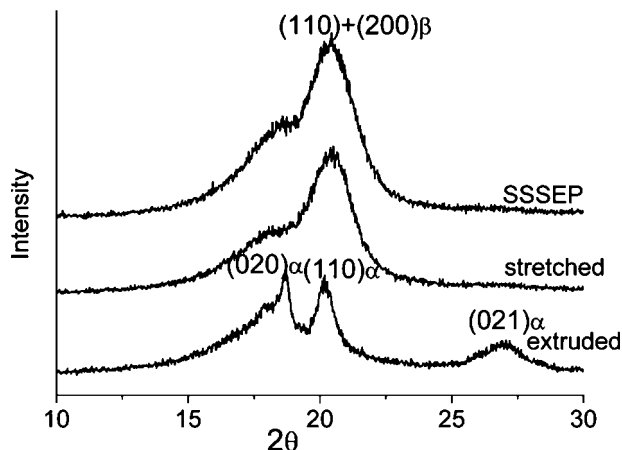


**Figure 3** WAXD patterns for extruded, stretched, and SSSEP films.

WAXD measurements were carried out from  $2\theta = 10^\circ$  to  $2\theta = 30^\circ$  as presented in Figure 3. The extruded films showed three clear peaks  $2\theta = 18.6^\circ$ ,  $2\theta = 20.1^\circ$ , and  $2\theta = 26.8^\circ$ , characterizing the (020), (110), and (021) reflections of  $\alpha$  phase, respectively.<sup>4,22</sup> However, the (100) reflection ascribing to  $\alpha$  phase of PVDF homopolymer was not detected, indicating that some  $\alpha$  phase transformed into  $\beta$  phase because of quenching in extrusion process, which is verified by FT-ATR [shown in Fig. 3]. The stretched films and SSSEP films showed similar profiles with a single peak at  $2\theta = 20.5^\circ$  and a shoulder at  $2\theta = 18.2^\circ$  which were assigned to the (110) (200) reflections of  $\beta$  phase and (020) reflection of  $\alpha$  phase, respectively, implying that neither stretching nor SSSEP can completely transform  $\alpha$  to  $\beta$  phase.

The crystalline and amorphous regions were separated by fitting the Gaussian function to calculate crystallinity, the results were 0.32, 0.34, and 0.39 for extruded, stretched and SSSEP films, respectively. It is showed that the SSSEP films possessed the highest crystallinity while the extruded films gave the lowest crystallinity, consistent with the DSC results of crystallization enthalpies. This implies that the SSSEP films have a perfect crystal structure in comparison with the stretched and extruded films.

FTIR-ATR can give useful information about the polymer structure, foregone studies showed that the vibration bands at 612, 763, 796, 855, 970, 1150, 1214, and 1383  $\text{cm}^{-1}$  correspond to  $\alpha$  phase,<sup>5-9</sup> whereas vibration bands at 840 and 1278  $\text{cm}^{-1}$  are the character bands of  $\beta$  phase.<sup>6,7,24</sup> From Figure 4, we can see that the extruded films showed the characteristic spectrum of the  $\alpha$  phase with absorption bands at 612, 763, 796, 855, 970, 1149, 1210, and 1383  $\text{cm}^{-1}$ , whereas there are also weak absorption at 840 and 1278  $\text{cm}^{-1}$ , suggesting that there is small amount of  $\beta$  phase in the extruded films. The stretched films and SSSEP films gave a similar pattern that 855, 1149, 1210, and 1383  $\text{cm}^{-1}$  were disappeared while the intensity of 612, 763, 796, and 970  $\text{cm}^{-1}$  were sharply decreased with

the increase of 840 and 1278  $\text{cm}^{-1}$ . These results reconfirmed the WAXD results that the extruded films mainly consisted of  $\alpha$  phase with a little amount of  $\beta$  phase, on the contrary, stretched, and SSSEP films mainly consisted of  $\beta$  phase with a little amount of  $\alpha$  phase.

The fraction of  $\beta$  phase can be calculated by using the following equation.<sup>5,9,10</sup>

$$F(\beta) = \frac{X_\beta}{X_\alpha + X_\beta} = \frac{A_\beta}{1.26A_\alpha + A_\beta} \quad (1)$$

Where  $X_\alpha$  and  $X_\beta$  are crystalline mass fraction of  $\alpha$  and  $\beta$  phase and the  $A_\alpha$  and  $A_\beta$  are their absorption bands at 763 and 840  $\text{cm}^{-1}$ , 1.26 is the ratio of absorption coefficients of  $K_\alpha$  and  $K_\beta$  at 763 and 840  $\text{cm}^{-1}$ . The calculated results were 0.12, 0.87, and 0.88 for the extruded, stretched, and SSSEP films, respectively. Using this method, our calculating results showed that the relative content of  $\beta$  in stretched and SSSEP films was almost the same, showing that poling has a little effect on increasing the ratio of transformation from  $\alpha$  to  $\beta$ .

Figure 5 gave the storage modulus ( $E'$ ) and the loss factor ( $\tan \delta = E''/E'$ ) for extruded films, stretched films, and SSSEP PVDF-HFP copolymer films, respectively. It is obviously that both the SSSEP and stretched films exhibited higher  $E'$  compared to the extruded films, moreover, the SSSEP films exhibited the highest  $E'$  among all the samples. This behavior seems to be related to different molecular chain orientation of the samples. Compared to the extruded films, the stretched and SSSEP films have higher molecular chain orientation in both crystalline and amorphous regions because of stretching, resulting in higher  $E'$ . In SSSEP films, dipoles orientation induced by poling increased the molecular chain reorientation, which in turn increased  $E'$ , compared with stretched films. The peak appeared at

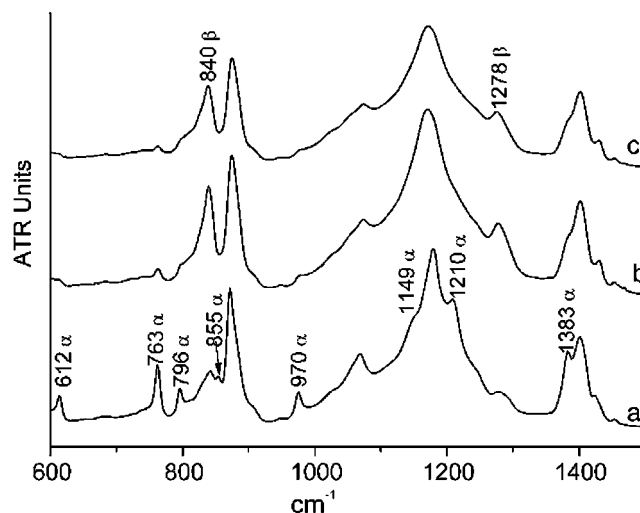


**Figure 4** FTIR-ATR spectra of PVDF-HFP copolymer films prepared under different conditions (a) extruded (b) stretched and (c) SSSEP.

$-40^{\circ}\text{C}$  in the  $\tan \delta$  curve corresponding to the glass transition, which was also called  $\beta$  or  $\alpha_a$  relaxation by other authors, was  $5^{\circ}\text{C}$  lower than the DSC results. Another peak in DSC results at  $50^{\circ}\text{C}$  also presented in the  $\tan \delta$  curve, which has been found in homolymer.<sup>25-28</sup> However, the cause of peak is uncertain, it maybe related to the level of constraint of part of the amorphous chains in the vicinity of crystalline domains<sup>26,27</sup> or condensation glass transition.<sup>28</sup> Recently, some authors attributed it to second crystallization induced by annealing or storage.<sup>25</sup>

### Piezoelectricity

Figure 6 showed the poling field dependencies of piezoelectric coefficient  $d_{33}$  for extruded, stretched, and SSSEP PVDF-HFP copolymer films. All films exhibited similar behavior with regard to the poling field, while the onset of the piezoelectric response of poling fields ( $E_0$ ) were different, 20 MV/m for both stretched and SSSEP films as well as 60 MV/m for extruded films. Among the three films, the SSSEP films exhibited the highest  $d_{33}$  at each poling field while the stretched films showed the second highest value, the extruded showed the lowest. The differences of  $E_0$  and  $d_{33}$  between extruded films and stretched or SSSEP films resulted from the different  $\beta$  phase content of the samples as discussed above, the lower  $\beta$  phase content of extruded films was responsible for the higher  $E_0$  and lowest  $d_{33}$ . It is interesting that although the stretched and SSSEP films have the similar crystallinity and  $\beta$  phase content, the  $d_{33}$  was obviously different. This distinction may be attributed to the different degree of  $\text{CF}_2$  dipole orientation towards the electric field in the two poling mode. In the SSSEP mode, the motion of molecular chain due to stretching made the  $\text{CF}_2$  dipole rotation active, so the electric field to orientate  $\text{CF}_2$  dipole is lower than the first stretched then poled

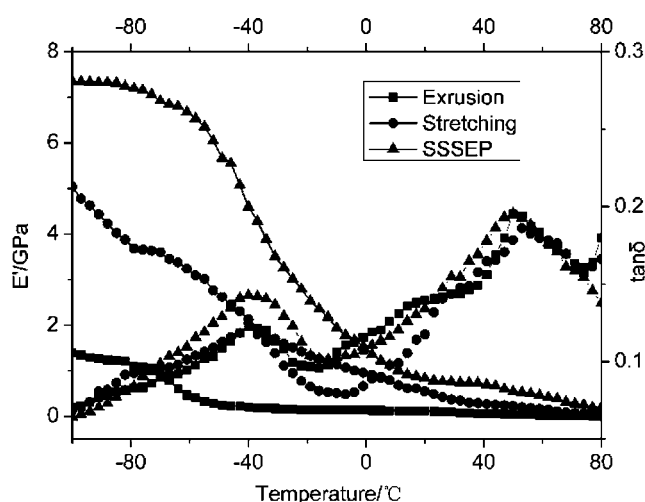


**Figure 5** DMA spectra for extruded, stretched, and SSSEP PVDF-HFP copolymer films.

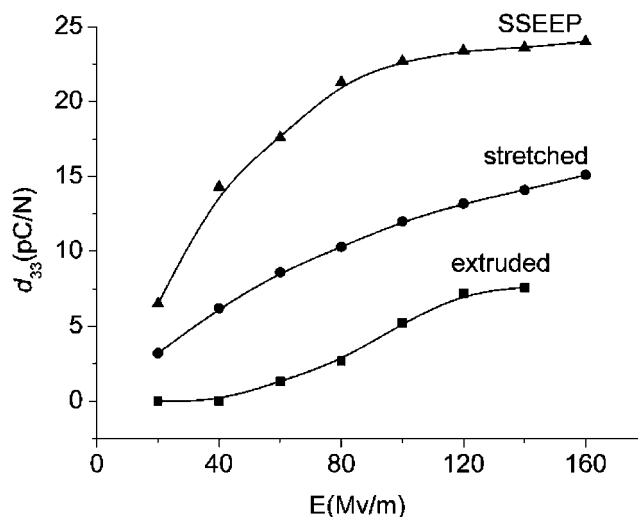


**Figure 6** Poling field dependence of piezoelectric coefficients  $d_{33}$  for extruded, stretched and SSSEP films.

mode, thus the former have higher degree of  $\text{CF}_2$  dipole than the latter resulting in the difference of the  $d_{33}$ . In other words, the potential energy for the rotation of the dipoles in the SSSEP mode is lower than the first stretched then poled mode. Moreover, the maximum  $d_{33}$  (24 pC/N) of SSSEP films at poling electric field of 160 MV/m is also higher than reported.<sup>29,30</sup>

### CONCLUSIONS

The influences of extrusion, stretching, and SSSEP on the properties of PVDF-HFP copolymer were studied with the help of DSC, WAXD, FTIR-ATR, and DMA. The extruded films exhibited the lowest crystallinity and  $\beta$  phase, while poled at high electric field it gave the lowest stress piezoelectric coefficient  $d_{33}$ . Although the stretched and SSSEP films showed similar  $\beta$  phase content,  $d_{33}$  was distinctly different at the same poling electric field. This distinction may be attributed to difference of the potential energy for the dipoles rotation which is lower in SSSEP mode than in the first stretched then poled mode. The SSSEP films also exhibited the highest modulus ( $E'$ ) among three films, indicating that SSSEP enhanced the chain orientation greatly compared with the stretching and extrusion methods. Furthermore, the maximum  $d_{33}$  of SSSEP films (24 pC/N) is higher than the other PVDF-HFP copolymer films that have been reported.

The authors acknowledge useful discussion on this work with Professor Xiaoniu Yang.

### References

1. Kawai, H. *Jpn J Appl Phys* 1969, 8, 975.
2. Furukawa, T. *Phase Transitions* 1989, 18, 43.
3. Kepler, G. R.; Anderson, R. A. *Adv Phys* 1992, 41, 1.

4. DasGupta, D. K.; Doughty, K. *Appl Phys Lett* 1977, 31, 585.
5. Salimi, A.; Yousefi, A. A. *J Polym Sci Part B: Polym Phys* 2004, 42, 3487.
6. Boccaccio, T.; Bottino, A.; Capannelli, G.; Piaggio, P. *J Membr Sci* 2002, 210, 315.
7. Gregorio, R., Jr. *J Appl Polym Sci* 2006, 100, 3272.
8. Zhang, G. Z.; Kitamura, H.; Yoshida, H.; Kawai, T. *J Therm Anal Calorim* 2002, 69, 939.
9. Gregorio, R., Jr.; Cestari, M. *J Polym Sci Part B: Polym Phys* 1994, 32, 859.
10. Salimi, A.; Yousefi, A. A. *Polym Test* 2003, 22, 699.
11. Sajkiewicz, P.; Wasiak, A.; Goclowski, Z. *Eur Polym J* 1999, 35, 423.
12. Davis, G. T.; McKinney, J. E.; Broashurst, M. G.; Roth, S. C. *J Appl Phys* 1978, 49, 4998.
13. Newman, B. A.; Yoon, C. H.; Pae, K. D.; Scheinbeim, J. I. *J Appl Phys* 1979, 50, 6095.
14. Yang, D.; Chen, Y. *J Mater Sci Lett* 1987, 6, 599.
15. Priya, L.; Jog, J. P. *J Polym Sci Part B: Polym Phys* 2003, 41, 31.
16. Guo, S.; Zhao, X. *Appl Phys Lett* 2004, 84, 3349.
17. Zhang, Q. M.; Bharti, V.; Zhao, X. *Science* 1998, 280, 2101.
18. Jayasuriya, A. C.; Schirolauer, A.; Scheinbeim, J. *J Polym Sci Part B: Polym Phys* 2001, 39, 2793.
19. Lu, X.; Schirolauer, A.; Scheinbeim, J. *IEEE Trans Ultrason Ferroelectr Freq Control* 2000, 47, 1291.
20. Künstler, W.; Wegener, M.; Seiß, M.; Gerhard-Multhaupt, R. *Appl Phys A* 2001, 73, 641.
21. Chung, N.; Kang, D.; Kim, D. *Polym Int* 2005, 54, 1153.
22. Abbrent, S.; Plestil, J.; Hlavata, D.; Lindgren, J.; Tegenfeldt, J.; Wendsjö, Å. *Polymer* 2001, 42, 1407.
23. Kaura, T.; Nath, R.; Periman, M. M. *J Phys D: Appl Phys* 1991, 24, 1848.
24. Benz, M.; Euler, W. B. *J Appl Polym Sci* 2003, 89, 1093.
25. Neidhöfer, M.; Beaume, F.; Ibos, L.; Bernès, A.; Lacabanne, C. *Polymer* 2004, 45, 1679.
26. Leonard, C.; Halary, J. L.; Monnerie, L.; Micheron, F. *Polym Bull* 1984, 11, 195.
27. El Mohajir, B.-E.; Heymans, N. *Polymer* 2001, 42, 5661.
28. Loufakis, K.; Wunderlich, B. *Macromolecules* 1987, 20, 2474.
29. Dargaville, T. R.; Celina, M.; Chapla, P. M. *J Polym Sci Part B: Polym Phys* 2005, 43, 1310.
30. He, X. J.; Yao, K.; Gan, B. K. *J Appl Phys* 2005, 97, 084101.